

Design and Fabrication of Freeform Holographic Optical Elements [Supplementary Document]

CHANGWON JANG, Facebook Reality Labs Research
 OLIVIER MERCIER, Facebook Reality Labs Research
 KISEUNG BANG, Facebook Reality Labs Research
 GANG LI, Facebook Reality Labs Research
 YANG ZHAO, Facebook Reality Labs Research
 DOUGLAS LANMAN, Facebook Reality Labs Research

ACM Reference Format:

Changwon Jang, Olivier Mercier, Kiseung Bang, Gang Li, Yang Zhao, and Douglas Lanman. 2020. Design and Fabrication of Freeform Holographic Optical Elements [Supplementary Document]. *ACM Trans. Graph.* 39, 6, Article 000 (2020), 3 pages. <https://doi.org/10.1145/1122445.1122456>

1 MODELING

1.1 Diffraction Efficiency Modeling

The selectivity an HOE is a function of the incident angle, the wavelength of light, and characteristics of the HOE material such as its thickness and refractive index modulation. We adopt the coupled wave theory (CWT) diffraction efficiency model of Yariv and Yeh [1983], which is known to match rigorous simulation results accurately. To calculate the diffraction efficiency, a wave equation is solved in a volume grating structure having refractive index n at position $r \in \mathbb{R}^3$:

$$n(r) = n_h + n_d \cos(\vec{K}_G \cdot \vec{r}), \quad (1)$$

where n_h is the refractive index of the HOE material and n_d is the amplitude of refractive index modulations. This model assumes the volume grating has a finite thickness in z , and is well approximated locally by a periodic function in x and y . With these assumptions, we can compute the diffraction efficiency η of reflective-type volume gratings to be

$$\eta = \|\kappa\|^2 \frac{\sinh(st)^2}{s^2 \cosh(st)^2 + \left(\frac{\Delta K}{2}\right)^2 \sinh(st)^2}, \quad (2)$$

where t is the thickness of the material, and

$$\kappa = \frac{2\pi n_d k_0}{\lambda \|\vec{K}_G\|}, \quad (3)$$

Authors' addresses: Changwon Jang, Facebook Reality Labs Research; Olivier Mercier, Facebook Reality Labs Research; Kiseung Bang, Facebook Reality Labs Research; Gang Li, Facebook Reality Labs Research; Yang Zhao, Facebook Reality Labs Research; Douglas Lanman, Facebook Reality Labs Research.

Permission to make digital or hard copies of all or part of this work for personal or classroom use is granted without fee provided that copies are not made or distributed for profit or commercial advantage and that copies bear this notice and the full citation on the first page. Copyrights for components of this work owned by others than ACM must be honored. Abstracting with credit is permitted. To copy otherwise, or republish, to post on servers or to redistribute to lists, requires prior specific permission and/or a fee. Request permissions from permissions@acm.org.

© 2020 Association for Computing Machinery.

0730-0301/2020/000-ART000 \$15.00

<https://doi.org/10.1145/1122445.1122456>

$$s = \sqrt{\|\kappa\|^2 - \left(\frac{\Delta K}{2}\right)^2}. \quad (4)$$

ΔK is the phase mismatch term (Equation 3 in our paper), λ is the wavelength, and k_0 is the norm of k -vectors in the medium. In practice, this expression is often approximated in previous works as a sinc function to get [Wissmann et al. 2008]

$$\eta_{\text{sinc}} = \tanh(\kappa t)^2 \sqrt{\text{sinc}\left(\frac{t\Delta K}{2\pi}\right)^2}. \quad (5)$$

However, these diffraction efficiency models require some modification to be used in our optimization because the side lobes in Equations 2 and 5 often causes the optimization to get stuck in a local minimum. To get rid of the side lobes, we can use a Gaussian function to approximate Equation 2 as

$$\eta_{\text{gaussian}} = \tanh(\kappa t)^2 \exp\left(-\left(\frac{t\Delta K}{2\pi}\right)^2\right), \quad (6)$$

which eliminates the local minima while retaining the same bandwidth and maximum diffraction efficiencies. However, the slope of this function can be very small when ΔK is large, and the iterations often fail to converge in a decent time. To prevent this, we propose to instead approximate the CWT model with a polynomial as

$$\eta_{\text{poly}} = \tanh(\kappa t)^2 \frac{1}{1 + \left(\frac{t\Delta K}{2\pi}\right)^4}. \quad (7)$$

Figure 1 shows the approximation models, as well as the selectivity optimization iterations for two different points on the HOE. In this example, the aspheric lens (Figure 10 in our paper) is set as the default HOE, and it is optimized to maximize efficiency for a normal incident ray bundle. The middle and right plots in Figure 1 show the iterations for locations (0 mm, 20 mm) and (0 mm, 25 mm) on the HOE, respectively. In the middle figure, the CWT model and sinc model get stuck in local minima, while the Gaussian approximation model and polynomial model successfully converge to the maximum efficiency. In the right figure, the CWT and sinc models get stuck at local minima and the Gaussian approximation also fails to converge due to its small slope, but our polynomial approximation model successfully converges.

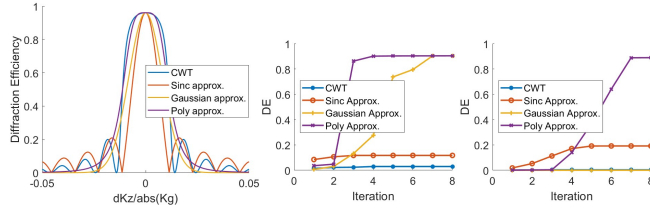


Fig. 1. Apodized diffraction efficiency modeling and optimization iterations to maximize the diffraction efficiency using the approximated models. Left: various approximations of the CWT diffraction efficiency function. Middle: The CWT model and its sinc approximation fail to converge due to local minima, while the Gaussian and polynomial approximations succeed to converge. Right: The Gaussian approximation also fails due to its gradient being too small, while our polynomial approximation is successful.

1.2 Basis Function Selection

Since the applications in this paper mainly concern HOEs with rectangular apertures, we use Legendre polynomials P_l with $l \in \mathbb{N}$ to represent the volume gratings. We use gradients of Legendre polynomials to represent b_{xn} , b_{yn} , and Legendre polynomials for b_{zn} (see Equation 5 in our paper). We have $P_0 = 1$ and $P_1 = x$, and Legendre polynomials can be computed recursively as

$$(m+1)P_{m+1}(x) = (2m+1)xP_m(x) - mP_{m-1}(x). \quad (8)$$

2D polynomials of order up to N can be described as a linear combination of 2D Legendre polynomial as

$$\sum_{l=0}^N \sum_{m=0}^l c_{lm} P_{l-m}(x) P_m(y) \quad (9)$$

for some coefficients c_{lm} . By defining $n = l(l-1)/2 + m$, the Legendre polynomials can be ordered to write the linear combination as a single sum, as we did in Equation 5 in our paper. For the z component, we define the n -th basis function b_{zn} as

$$b_{zn}(x, y) = P_{l-m}(x) P_m(y). \quad (10)$$

For the x and y components, we define the n -th basis functions $b_{xn}(x, y)$ and $b_{yn}(x, y)$ from gradients of the Legendre polynomials as

$$b_{xn}(x, y) = \frac{\partial}{\partial x} P_{l-m}(x) P_m(y), \quad (11)$$

$$b_{yn}(x, y) = \frac{\partial}{\partial y} P_{l-m}(x) P_m(y). \quad (12)$$

We use gradients of polynomials for x and y because it corresponds to using Legendre polynomials for the optical phase of the HOE, and helps convergence in practice. We use polynomials of up to sixth order in our examples, which is at most 21 basis functions. This is small enough to make computation times reasonable while still converging to an accurate solution.

We note that the type of basis function does not have a large effect on the optimization results, provided that they can model a smooth phase profile. We have tested Zernike and Fourier basis functions and obtained similar optimization results. It is therefore convenient to simply use the type of basis function that matches the

HOE shape (Legendre for rectangular domains, Zernike for circular domains).

2 DETAILS OF HOE CONFIGURATIONS

2.1 Freeform HOEs

We give here a more detailed description of the HOE configurations used for the optimization of Section 3.2. Rays are generated at a source, such as a display panel, and form an image at the sensor plane. The optimization of the HOE is initialized from a baseline HOE using simple spherical and plane wave conjugates. Each HOE element in our designs has a fixed aperture of 50 mm \times 50 mm.

Tracing rays from the source to the sensor plane seems natural, but since the exit pupil of the system is usually located at the sensor plane, it is significantly easier to trace the rays backward from the sensor to the source to make sure the rays pass through the exit pupil. Rays are traced in bundles with the same direction but different starting locations on the sensor plane. For the HUD system example, we use 7×7 ray bundles of 20×20 ray each. The rays are traced sequentially while tracking the intensity along the ray, and they are collected at the source plane where their PSF is computed.

This ray tracing framework is convenient to apply our optimization process to a broad range of designs. For example, fixed refractive elements and mirror surfaces can easily be added as part of the ray path, and their position and orientation can be added as variables in the optimization process, if desired.

Our optimization process typically converges within 40 iterations for our single HOE designs, and within 170 iterations for our example using two HOEs.

Each configuration in Figure 10 of the paper is detailed as follows:

- **Aspheric lens:** The camera distance is 100 mm, the focal length is 60 mm. Both the camera and the HOE are in the normal direction. The wavelength is 532 nm.
- **HUD lens:** The camera distance is set to 200 mm, the panel distance is 100 mm at a 45 degree angle. The wavelength is 532 nm. We note that the specifications used for the holographic printer are slightly different due to the bandwidth limitations of the holographic printer: the camera distance is changed to 225 mm, and the panel distance is changed to 150 mm.
- **HUD doublet:** The camera distance is 150 mm, the first HOE is tilted by 22.5 degrees, the second HOE is tilted by 11.25 degrees, and the panel is tilted by -11.25 degrees. The second HOE is located at (0, -45 mm, -45 mm) and the panel is at (0, -53 mm, -5.8 mm). The wavelength is 532 nm.
- **Lens array:** The camera distance is 150 mm with a 45 degree angle, and the object distance is 200 mm. Seven lenslets are designed separately, with their centers at (0 mm, 0 mm), (0 mm, -12 mm), (0 mm, 12 mm), (-7 mm, -6 mm), (7 mm, -6 mm), (-7 mm, 6 mm), and (7 mm, 6 mm) on the HOE. The wavelength is 660 nm.

2.2 Caustic HOEs

We note that the diamond turning method is more appropriate for fabricating caustic HOEs because the hogel structure of printed HOEs creates diffracted patterns when projected at a large distance.

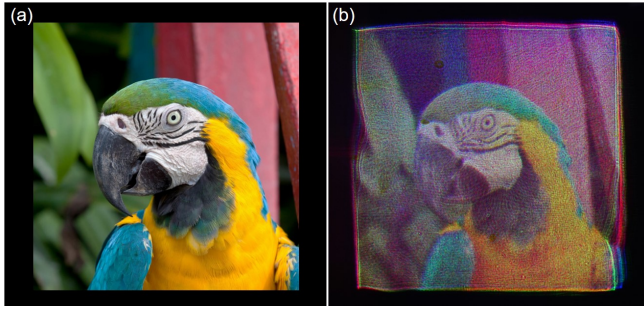


Fig. 2. (a) The target image and (b) the caustic projection result using our fabricated caustic HOE.

In the caustic HOE example in Figures 8 and 9, the image distance is set to 500 mm, and the size of the projected image is set to 220 mm. The illumination is set as a point light source located at 180 mm incident at a 45 degree oblique angle. The diamond-turning approach was used to fabricate the full-color parrot caustic HOE. For the full-color parrot caustic, the image distance is set to 600 mm and the image size is set to 200 mm. The illumination is set as a plane wave incident at a 45 degree oblique angle. Figure 2 (a) shows the target image used for caustic optimization and (b) shows the experimental result.

REFERENCES

- Patrick Wissmann, Se Baek Oh, and George Barbastathis. 2008. Simulation and optimization of volume holographic imaging systems in Zemax®. *Optics express* 16 (06 2008), 7516–24.
- Amnon Yariv and Pochi Yeh. 1983. *Optical waves in crystals: propagation and control of laser radiation*.